JCB Article

# Barrier-to-autointegration factor: major roles in chromatin decondensation and nuclear assembly

**Miriam Segura-Totten,[1] Amy K. Kowalski,[1] Robert Craigie,[2] and Katherine L. Wilson[1]**

[1]Department of Cell Biology, The Johns Hopkins University School of Medicine, Baltimore, MD 21205
[2]Laboratory of Molecular Biology, National Institute of Diabetes and Digestive and Kidney Diseases, National Institutes of Health, Bethesda, MD 20892

Barrier-to-autointegration factor (BAF) is a DNA-bridging protein, highly conserved in metazoans. BAF binds directly to LEM (LAP2, emerin, MAN1) domain nuclear membrane proteins, including LAP2 and emerin. We used site-directed mutagenesis and biochemical analysis to map functionally important residues in human BAF, including those required for direct binding to DNA or emerin. We also tested wild-type BAF and 25 point mutants for their effects on nuclear assembly in *Xenopus* egg extracts, which contain ~12 μM endogenous BAF dimers. Exogenous BAF caused two distinct effects: at low added concentrations, wild-type BAF enhanced chromatin decondensation and nuclear growth; at higher added concentrations, wild-type BAF completely blocked chromatin decondensation and nuclear growth. Mutants fell into four classes, including one that defines a novel functional surface on the BAF dimer. Our results suggest that BAF, unregulated, potently compresses chromatin structure, and that BAF interactions with both DNA and LEM proteins are critical for membrane recruitment and chromatin decondensation during nuclear assembly.

Downloaded from www.jcb.org on February 7, 2006

## Introduction

Barrier-to-autointegration factor (BAF)* is a DNA-bridging protein with a dimer mass of 20 kD, which is highly conserved in metazoans (Cai et al., 1998). BAF is not homologous to any known proteins, but has a helix–hairpin–helix structural motif (Umland et al., 2000) conserved among proteins that bind nonspecifically to DNA (Shao and Grishin, 2000). BAF was first discovered as an activity in NIH3T3-cell cytosol that prevents reverse-transcribed retroviral DNA from undergoing suicidal autointegration (Chen and Engelman, 1998; Lee and Craigie, 1998). BAF dimers are proposed to associate with viral preintegration complexes in vivo, and noncovalently crossbridge viral DNA (Lee and Craigie, 1998). Biochemical analysis showed that BAF dimers bind nonspecifically to double-stranded DNA (dsDNA); BAF does not bind RNA or single-stranded DNA (Zheng et al., 2000). However, the conserved function of BAF in uninfected cells was not known.

In a two-hybrid screen (Furukawa, 1999), BAF was found to interact with lamin associated polypeptide (LAP)2β, a nuclear inner membrane protein (Foisner and Gerace, 1993). Furthermore, BAF appeared to localize predominantly on chromatin in the nucleus (Furukawa, 1999), suggesting that BAF might function in the nucleus, despite its original purification from NIH3T3-cell cytosol (Lee and Craigie, 1998). LAP2β is an abundant nuclear membrane protein with an ~40-residue motif known as the LEM (LAP2, emerin, MAN1) domain. The LEM domain defines a growing family of nuclear membrane proteins (Lin et al., 2000), whose members include multiple splicing isoforms of LAP2 (Berger et al., 1996; Gant et al., 1999), plus emerin, MAN1 (Lin et al., 2000), Lem-3 (Lee et al., 2000), and otefin (Goldberg et al., 1998). Site-directed mutagenesis studies of LAP2 (Shumaker et al., 2001) and emerin (Lee et al., 2001) show that the LEM motif is essential for binding to BAF and to BAF–DNA complexes. LEM domain structure, solved by NMR (Cai et al., 2001; Wolff et al., 2001), complements both the shape and hydrophobicity of a surface on the BAF dimer (Umland et al., 2000). Importantly, BAF can bind simultaneously to both LAP2 and DNA in vitro (Shumaker et al., 2001), suggesting that BAF might play a key role in attaching chromatin to the inner nuclear membrane. In addition, both LAP2β and emerin interact with nuclear

The online version of this article contains supplemental material.

Address correspondence to Katherine L. Wilson, Dept. of Cell Biology, The Johns Hopkins University School of Medicine, 725 N. Wolfe St., Baltimore, MD 21205. Tel.: (410) 955-1801. Fax: (410) 955-4129. E-mail: klwilson@jhmi.edu

*Abbreviations used in this paper: BAF, barrier-to-autointegration factor; CD, circular dichroism; dsDNA, double-stranded DNA; hBAF, human BAF; LAP, lamin-associated polypeptide; LEM, LAP2, emerin, MAN1; NPC, nuclear pore complex; TEM, transmission electron microscopy.

Key words: HIV; retroviral preintegration complex; nucleus; emerin; nuclear envelope

© The Rockefeller University Press, 0021-9525/2002/08/475/11 $5.00
The Journal of Cell Biology, Volume 158, Number 3, August 5, 2002 475–485
http://www.jcb.org/cgi/doi/10.1083/jcb.200202019

Supplemental Material can be found at:
http://www.jcb.org/cgi/content/full/jcb.200202019/DC1

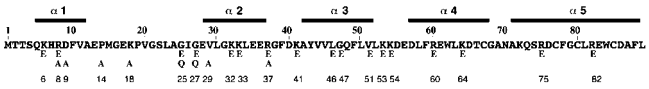


Figure 1. **BAF mutagenesis.** Residues that comprise the five α-helices in BAF are indicated by bars above the amino acid sequence of human BAF (Umland et al., 2000; Cai et al., 2001). Point mutations are indicated by E (glutamic acid), Q (glutamine), and A (alanine), and numbered. Each BAF mutant contained one substituted residue. A few residues were changed to either of two mutant residues.

intermediate filament proteins named lamins (Foisner and Gerace, 1993; Clements et al., 2000; Vaughan et al., 2001), which comprise a key structural element of the nucleus and play critical roles in nuclear assembly (for review see Stuurman et al., 1998; Cohen et al., 2001). Collectively, these results suggest an important hypothesis: by binding to LEM proteins, BAF might link chromatin directly to the inner nuclear membrane and indirectly to lamin filaments. This model predicts that BAF may be essential for nuclear assembly, or for the structural integrity of interphase nuclei, or both.

In this study, we used site-directed mutagenesis to define and map functionally important surfaces on the BAF dimer. Through biochemical assays, we identified residues required for BAF to bind to DNA or emerin, and residues important for BAF dimer interactions. We then tested wild-type human BAF protein and our 25 point mutants for their effects on nuclear assembly in *Xenopus* egg extracts (Lohka and Masui, 1983; Wilson and Newport, 1988). The wild-type and mutant BAF proteins fell into four classes with respect to their nuclear assembly phenotypes, and were interpreted based on the biochemical activities of each mutant. Our results support the hypothesis that BAF has fundamental roles during nuclear assembly, and that BAF interactions with both DNA and LEM proteins are critical for chromatin decondensation and nuclear envelope growth.

## Results

We used site-directed mutagenesis to make point mutations throughout the human BAF protein (Fig. 1). Twelve charged residues were changed to the opposite sign, charges were introduced at seven sites, and six residues exposed to solvent in the BAF dimer (Umland et al., 2000) were replaced by alanine. All 25 His-tagged mutant proteins were expressed and purified from bacteria (see Materials and methods). These point mutants were used to identify residues in BAF required to bind emerin or DNA, and to examine interactions between wild-type and mutant BAF proteins.

Table I. **Summary of mutant BAF protein properties**

| Nuclear assembly phenotype | Mutation | Binds emerin? | Binds DNA? |
|---|---|---|---|
| **Wild-type** | WT | + | + |
| | 6E | +/− | −/+ |
| | 8A | + | + |
| | 8E | + | + |
| | 29A | + | + |
| | 32E | + | + |
| | 33E | + | + |
| | 37A | + | + |
| | 37E | + | + |
| | 51E | − | +/− |
| | 54E | − | +/− |
| | 60E | + | + |
| | 75E≠ | +/− | +/− |
| | 82E | + | + |
| **Inactive** | 25E | − | − |
| | 25Q | − | +/− |
| | 27E | +/− | −/+ |
| | 27Q | +/− | +/− |
| | 46E | − | − |
| **Always condensed** | 14A | + | + |
| | 18A | + | + |
| | 47E | − | + |
| **Inactive to condensed** | 9A | +/− | +/− |
| | 41E | + | + |
| | 53E | − | + |
| | 64E | + | + |

(+) wild-type activity; (+/−) reduced activity; (−/+) severely reduced activity; (−) undetectable activity, (≠) behaves like wild-type in nuclear assembly, but DNA at the nuclear poles is clumped.

### Residues in BAF required for emerin binding

To identify residues required for binding to emerin, we tested the binding of wild-type and mutant BAF proteins to blot-immobilized recombinant emerin residues 1–222, comprising the full nucleoplasmic domain (Lee et al., 2001; see Materials and methods). Each BAF protein was $^{35}$S labeled in coupled transcription–translation reactions, and used to probe human emerin on blots (Fig. 2). Seven mutants (25E, 25Q, 46E, 47E, 51E, 53E, and 54E) showed little or no detectable binding to emerin, and six (6E, 8E, 9A, 27E, 27Q, and 75E) had consistently reduced binding (Fig. 2), relative to the amount of each input probe (unpublished data), as summarized in Table I. Three residues essential for binding to emerin clustered in a concave valley (see below) that complements the LEM domain (see Discussion).

### Mutations in BAF that affect DNA binding

BAF binding to DNA was previously tested using gel-shift assays and short (21-bp) pieces of DNA (Harris and Engelman, 2000; Umland et al., 2000; Zheng et al., 2000; Shu-

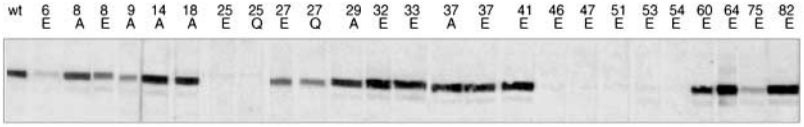


Figure 2. **Binding of mutant hBAF proteins to blot-immobilized emerin.** Blots bearing human emerin protein (residues 1–222) were cut into strips. Each strip was probed with $^{35}$S-labeled wild-type or mutant BAF, numbered as in Fig. 1. Radiolabeled wild-type human BAF (WT) served as a positive control. Binding of each mutant BAF to emerin was scored relative to the amount of each input probe (unpublished data), and summarized in Table I.

Downloaded from www.jcb.org on February 7, 2006

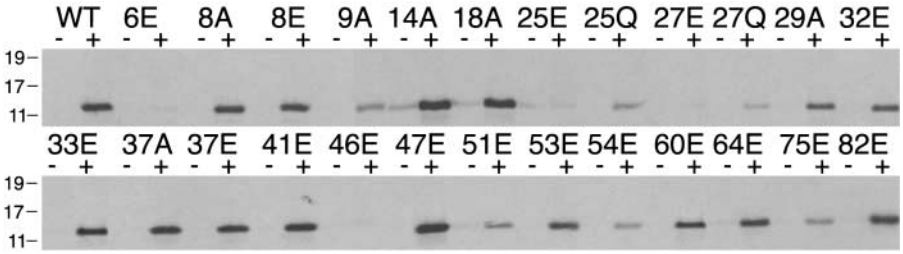


Figure 3. **DNA binding activity of BAF mutants.** Each $^{35}$S-labeled wild-type or mutant BAF protein was incubated with (+) or without (−) native DNA cellulose beads, then pelleted, washed, separated on SDS-PAGE, and detected by autoradiography.

maker et al., 2001). Nearly all tested mutations disrupted binding to short DNA. By contrast, we examined BAF binding to longer pieces of dsDNA (200–6,000 bp) using native DNA-cellulose beads. Wild-type and mutant $^{35}$S-labeled BAF proteins were each incubated for 2 h in the presence (+) or absence (−) of DNA-cellulose beads, to control for possible DNA-independent BAF aggregation. Samples were washed, and pelleted proteins were subjected to SDS-PAGE and autoradiographed. Four mutants (6E, 25E, 27E, and 46E) had severely reduced or undetectable DNA binding activity, and six (9A, 25Q, 27Q, 51E, 54E, and 75E) had reduced DNA binding activity (Fig. 3). The remaining mutants were indistinguishable from wild-type. Residues critical for DNA binding were consistent with predictions from the BAF crystal structure (Umland et al., 2000; see below).

Unexpectedly, all mutations that disrupted binding to DNA also reduced binding to emerin (Table I), suggesting that these mutations might cause misfolding. Therefore, we tested a subset of all our mutants (14A, 25E, 41E, 47E, and 53E) by circular dichroism (CD) to measure α-helix integrity, and by size exclusion chromatography to assess dimer formation (unpublished data). Mutants 14A, 41E, and 47E folded as well as wild-type, ruling out misfolding. Mutants 25E and 53E had a slight decrease in helical content, but otherwise had CD spectra similar to wild-type BAF, indicating no gross disruption of secondary structure. Size exclusion on Sephadex 25 columns, which discriminate 10-kD monomers and 20-kD dimers, showed that wild-type BAF eluted as two peaks, as expected: one with a retention time indicative of dimers, plus a higher molecular weight aggregate (Cai et al., 1998; Harris and Engelman, 2000). Mutants 14A, 41E, and 53E clearly had a major dimer peak, like wild-type BAF. There was no dimer peak for mutant 25E; instead, there was some larger aggregate and a peak that eluted slightly slower than dimers, suggesting that mutant G25E does not form normal dimers. Mutant 47E had a dimer peak. This was surprising because residue 47 maps to α-helix 3, and was predicted to disrupt dimerization. Based on these assays, we concluded that mutants 14A, 41E, 53E, and, surprisingly, 47E, were folded and formed homodimers as well as wild-type BAF. In contrast, mutant 25E was not grossly disordered but failed to form homodimers. Gly-25 mediates a tight turn between helices 1 and 2, and changing this residue to glutamate may stiffen the polypeptide backbone, in addition to introducing a negative charge.

We did one further assay, to anticipate the behavior of each BAF mutant when added to *Xenopus* extracts containing wild-type *Xenopus* BAF. Selected His-tagged BAF mutants were incubated with equal amounts of $^{35}$S-labeled wild-type BAF and then immunoprecipitated using anti-His antibodies (Fig. 4, A and B). This subunit exchange assay tested the ability of wild-type $^{35}$S-BAF dimers (and/or oligomers) to exchange or oligomerize with BAF mutants. Compared with wild-type BAF, we expected that mutants with weaker dimer interactions would exchange more frequently with $^{35}$S-labeled wild-type BAF. The wild-type control showed relatively low (ratio $\sim$ 0.1) levels of subunit exchange or oligomerization with wild-type $^{35}$S-BAF (Fig. 4 C, left). The same low signal was seen for mutants 25E and 41E (Fig. 4 C, left) and 14A (Fig. 4 C, right), relative to input His-tagged wild-type BAF. Note that a low signal was consistent with either (a) stable dimerization with no exchange of subunits, or (b) complete failure to dimerize or oligomerize. Slightly higher signals were seen for mutants 18A, 53E, 54E, and 75E, but this difference may not be significant. However, wild-type $^{35}$S-BAF exchanged at abnormally high levels with mutants 47E and 51E (Fig. 4 C). We concluded that mutants 47E and 51E had

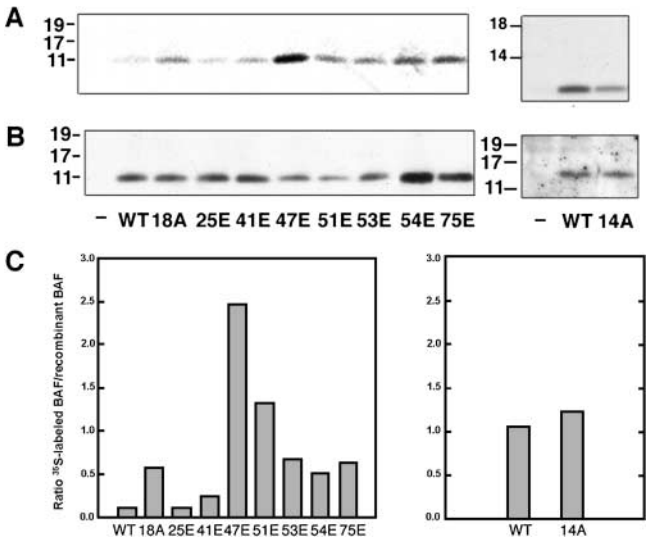


Figure 4. **Subunit exchange assay.** Each His-tagged mutant BAF protein was incubated with $^{35}$S-labeled wild-type BAF, and immunoprecipitated with anti-His antibody. As positive and negative controls, $^{35}$S-wild-type BAF was incubated with (WT) or without (−) His-tagged wild-type BAF, respectively, before immunoprecipitation and SDS-PAGE. The left and right panels are from different experiments, and had different amounts of input $^{35}$S-wild type BAF. (A) Autoradiographs showing the $^{35}$S-labeled wild-type BAF that coimmunoprecipitated with wild-type BAF (WT), or each BAF mutant (numbered as in Fig. 1). (B) Parallel Western blots probed with anti-His antibody, showing the amount of His-tagged BAF present in each reaction. All recombinant proteins migrated at their expected mass of 10 kD. (C) Densitrometric ratios of signals shown in A and B. Graphs show relative amounts of $^{35}$S-wild-type BAF that interacted with each input His-tagged BAF.

Downloaded from www.jcb.org on February 7, 2006

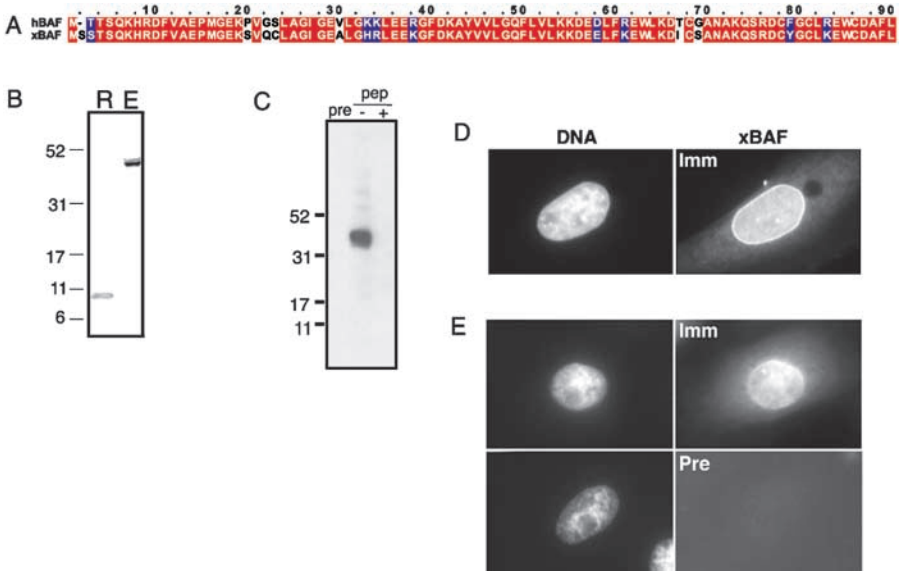


Figure 5. **Cloning, expression, and localization of *Xenopus* BAF.** (A) Human (top) and *Xenopus* (bottom) BAF are 84% identical (red) and 91% similar (blue). (B) Affinity-purified rabbit antibodies (serum 3710) recognized both recombinant (*R*) and endogenous (*E*) *Xenopus* BAF. Recombinant BAF (calculated mass, 10.2 kD) migrated at 10 kD on SDS-PAGE, whereas endogenous BAF migrated at 40 kD. (C) Western blot of the soluble fraction of *Xenopus* egg extracts showing that recognition of endogenous BAF by affinity-purified 3710 antibody was specifically competed by pretreatment (+) with antigenic peptide. Pre, preimmune antibody; pep, antigenic peptide. (D and E) Indirect immunofluorescent staining of endogenous BAF in cultured *Xenopus* A6 cells (D) and XLK-WG cells (E) using affinity-purified immune (Imm) or preimmune (pre) 3710 antibody. xBAF localizes predominantly at the nuclear rim, but is also found in the nuclear interior and cytosol (D and E, right). Left panels show DNA in the same cells, stained by Hoechst 33258.

high potential to exchange subunits (forming heterodimers or heterooligomers) with wild-type BAF, and that other mutants (18A, 53E, 54E, and 75E) had a slightly increased potential. The surprising result was that mutants 51E and 47E, which map to α-helix 3 and were predicted not to dimerize (Umland et al., 2000), can form homodimers and weak heterodimers/heterooligomers with wild-type BAF. However, another surface of BAF, distinct from helix 3, and not affected by mutations 47E and 51E, might independently mediate dimer or oligomer interactions.

## Characterization of *Xenopus* BAF

To test our hypothesis that BAF might function during nuclear assembly, we wanted to add exogenous BAF to nuclear assembly reactions in *Xenopus* egg extracts, which contain endogenous LEM proteins (Gant et al., 1999) and endogenous BAF (see below). We first cloned *Xenopus* BAF (xBAF), which is 84% identical and 91% similar to human BAF (Fig. 5 A). Affinity-purified antibodies against a *Xenopus*-specific BAF peptide (residues 19–35) specifically recognized bacterially expressed recombinant xBAF as an ~10-kD protein on blots of SDS gels (Fig. 5 B, Recombinant), as expected. This same antibody predominantly recognized a ~40 kD protein on immunoblots of the soluble fraction of *Xenopus* eggs (Fig. 5 B, Endogenous). This 40-kD band was not recognized by preimmune serum (Fig. 5 C, pre), and immune recognition was specifically competed by the antigenic peptide (Fig. 5 C, + pep). This 40-kD band probably represents a disulfide-bridged aggregate formed during cell lysis and boiling in SDS sample buffer, because BAF is highly sensitive to oxidation and contains four cysteines. When stained by indirect immunofluorescence in cultured *Xenopus* epithelial (A6) cells, BAF localized diffusely in the nucleus, and was enriched at the nuclear envelope (Fig. 5, D and E), supporting our hypothesis that BAF mediates chromosome attachment to membrane-bound LEM proteins. The intranuclear signal was consistent with BAF binding to intranuclear LEM proteins, such as LAP2α (Dechat et al., 2000). The same localizations were seen in an independent line of *Xenopus* kidney cells (XLK-WG) stained with affinity-purified immune (Fig. 5 E, Imm) and preimmune (Fig. 5 E, Pre) antibodies. Importantly, these experiments also revealed a low but reproducible signal for BAF in the cytoplasm (Fig. 5 E; see Discussion).

## Wild-type BAF can enhance or block chromatin decondensation in assembling nuclei

To test for possible roles in nuclear assembly, we added recombinant wild-type *Xenopus* BAF protein to *Xenopus* nuclear assembly reactions, which consist of fractionated egg cytosol and membranes, plus demembranated sperm chromatin (see Materials and methods). For simplicity, we assumed that our recombinant BAF proteins were all dimers. Nuclei were assembled for two hours, then stained for DNA and imaged by light microscopy. The no-addition control nuclei assembled normally and had decondensed chromatin (Fig. 6 A, 0 μM BAF). Added wild-type xBAF caused two opposite effects, depending on its concentration. With 0.5 μM added xBAF dimers, nuclei were larger and appeared to have enhanced chromatin decondensation (Fig. 6 A). With higher levels of added xBAF (2.5 to 5 μM), the chromatin remained small (condensed phenotype). We concluded that excess BAF might saturate its endogenous binding partners or regulators, allowing BAF to act in an unregulated DNA-bridging manner. Human BAF gave the same results, including better enhancement of chromatin decondensation at 0.5 μM (Fig. 6 B).

We next viewed the timecourse of nuclear assembly in the presence of 0 or 5 μM added xBAF (Fig. 6 C). The condensed phenotype was established early; the sperm chroma-

Downloaded from www.jcb.org on February 7, 2006

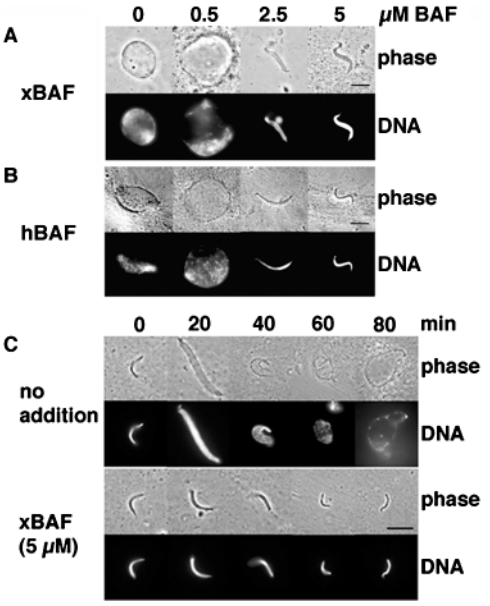


Figure 6. **Exogenous BAF has two distinct effects on chromatin when added to *Xenopus* nuclear assembly reactions.** Purified recombinant *Xenopus* BAF (A) or human BAF (B) were added to *Xenopus* nuclear assembly reactions at time zero, at concentrations of 0, 0.5, 2.5, or 5 μM recombinant BAF dimers. (A–C) Upper panels show nuclei by phase contrast microscopy; corresponding lower panels show same nuclei stained for DNA with Hoechst 33258. Nuclei were imaged after 2 h of assembly. (C) Timecourse (20-min intervals) of nuclear assembly without (no addition), or with 5 μM exogenous xBAF dimers (xBAF). Bars: (A and B) 10 μm; (C) 30 μM.

tin failed to either swell (an ionic effect; Philpott et al., 1991, see 20-min timepoint) or decondense, and appeared to compress further over time (Fig. 6 C). We hypothesized that the condensed phenotype might be due to excess BAF (a) blocking membrane binding to chromatin, (b) dominantly compressing chromatin, or (c) both.

To determine if exogenous BAF also disrupted intact (preassembled) nuclei, we assembled nuclei in *Xenopus* extracts for 1 h, and then added 0.5 or 5 μM BAF dimers. Exogenous BAF had no obvious effect on chromatin or nuclear growth, relative to buffer-treated controls (unpublished data). However, this does not rule out roles for BAF in interphase nuclear structure or function, because we do not know if exogenous BAF can disrupt preassembled endogenous BAF complexes.

## Transmission electron microscopy analysis of BAF-arrested nuclei

When imaged by transmission electron microscopy (TEM) after 2 h of assembly, the control (no addition) nuclei had typical nuclear membranes with nuclear pore complexes (NPCs) (Fig. 7 A, NPCs marked by asterisks). In contrast, nuclei arrested by 5 μM added BAF had patches of double membranes separated by gaps (Fig. 7 B, arrow), and areas devoid of membrane (Fig. 7 B). However, the most prominent abnormalities in these condensed nuclei involved chromatin. There was a compressed outer shell of electron-dense chromatin (Fig. 7 B, paired arrowheads) that appeared to encapsulate the interior chromatin. Indirect immunofluorescence with a lamin-specific antibody showed that this outer shell did not include lamins (Fig. S1 D, available at http://www.jcb.org/cgi/content/full/jcb.200202019/DC1). BAF was detected on these nuclei by immunofluorescence, concentrated at the periphery (Fig. S1 B, available at http://www.jcb.org/cgi/content/full/jcb.200202019/DC1). Furthermore, the interior chromatin had a novel lattice-like morphology (Fig. 7 B). This lattice morphology was not seen in the sperm chromatin template (Fig. 7 C), or in chromatin of GTPγS-arrested nuclei (Boman et al., 1992). These dominant effects of BAF on chromatin structure during nuclear assembly are novel and exciting. We hypothesized that the outer shell of condensed chromatin and interior lattice were due to unregulated DNA-bridging activity of excess BAF.

To interpret the concentration-dependent effects of BAF, it was critical to know how much endogenous BAF is present in the soluble and membrane fractions of *Xenopus* eggs. An affinity-purified anti-peptide antibody (serum 3710) was used to detect BAF by western blotting (see Materials and methods). BAF was present only in the soluble fraction (unpublished data), suggesting that BAF is released from membrane-bound LEM proteins during mitosis. The endogenous concentration of BAF monomers in *Xenopus* extracts is 25 μM (12.5 μM dimeric BAF), based on titrating *Xenopus* cytosol against known amounts of recombinant xBAF on blots (unpublished data; see Materials and methods). Because BAF is an essential protein (unpublished data), its abundance in *Xenopus* cytosol is no surprise. *Xenopus* eggs are also stockpiled with histones, polymerases and nucleoporins, which enable rapid cell divisions in early embryos (Woodland and Adamson, 1977; Meier et al., 1995).

Downloaded from www.jcb.org on February 7, 2006

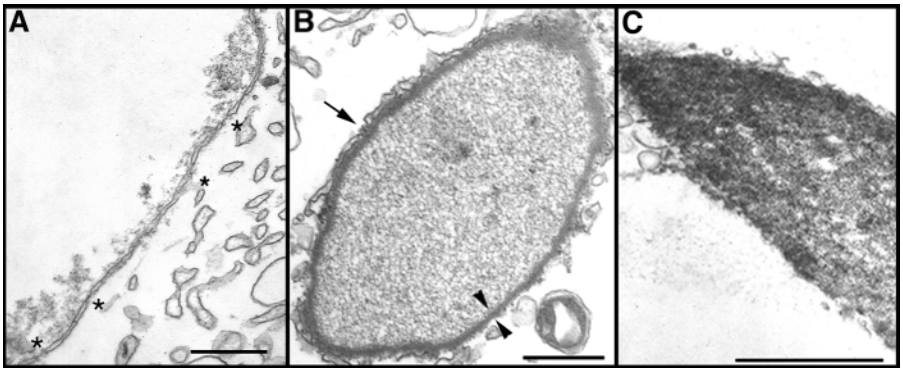


Figure 7. **Transmission EM of control and wild-type xBAF-inhibited nuclei.** Nuclei were assembled for 2 h with no BAF added (A) or 5 μM added xBAF dimers (B), and visualized by TEM. (A) Asterisks indicate nuclear pore complexes. (B) Nuclei assembled in 5 μM xBAF had patches of membranes at the chromatin surface. Arrow indicates chromatin emerging between membrane patches. Paired arrowheads bracket the electron-dense outer shell of chromatin in inhibited nuclei. (C) TEM cross-section of sperm chromatin before addition to assembly extracts. Bars, 500 nm.

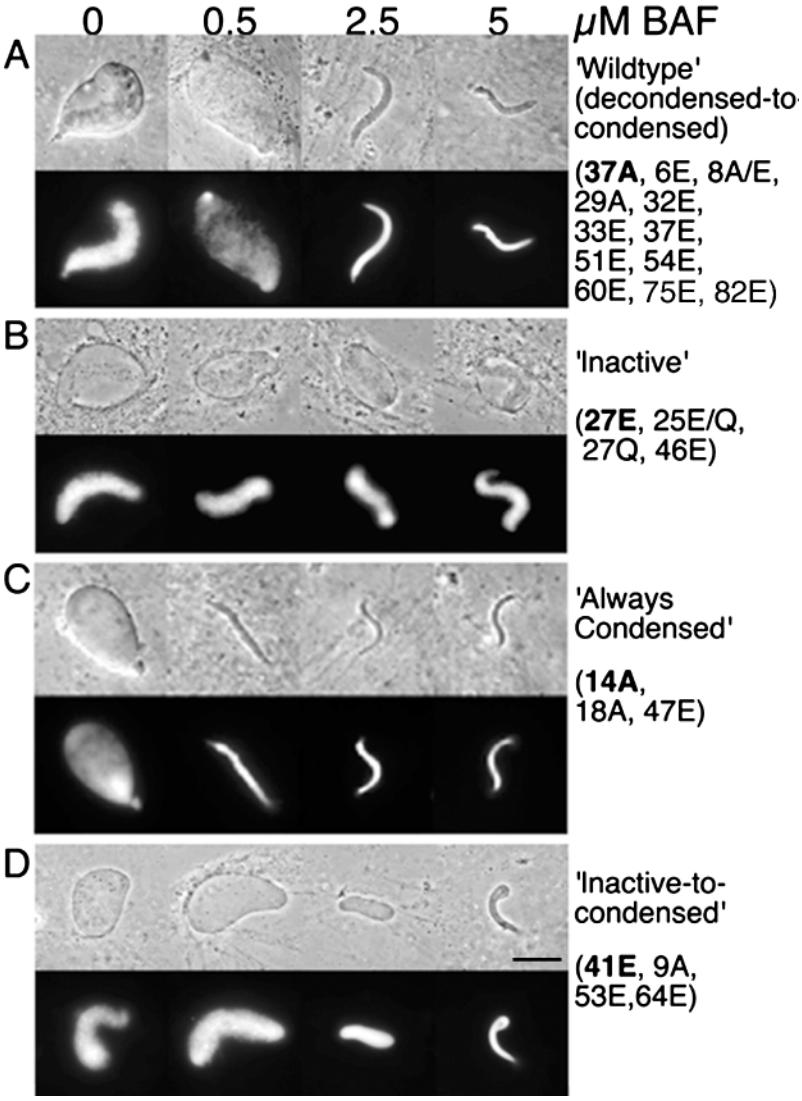


Figure 8. **Effects of mutant hBAF proteins on nuclear assembly in *Xenopus* egg extracts.** Mutant BAF proteins were added at time zero to the indicated final concentrations, and imaged after 2 h of assembly. Mutants fell into four phenotypes by light microscopy: (A) wild-type (decondensed-to-condensed), (B) inactive, (C) always condensed, and (D) inactive-to-condensed. The representative mutant shown for each class is bolded. Mutants are numbered according to Fig. 1. Mutant 75E behaved like wild-type BAF, but with clumps of DNA at the nuclear poles. Bar, 10 μm.

Downloaded from www.jcb.org on February 7, 2006

Given that *Xenopus* extracts contain about 12.5 μM endogenous BAF dimers, we reinterpreted Figs. 6 and 7 as follows. Increasing the total BAF concentration in *Xenopus* extracts by only 4% (adding 0.5 μM xBAF dimers) enhanced chromatin decondensation and nuclear growth, suggesting a positive role for BAF in nuclear assembly. However, increasing BAF by 20% (adding 2.5 μM xBAF) compacted chromatin and blocked nuclear growth. The strong dominant effects of 20% extra BAF suggested that BAF is normally regulated by binding partners that are stoichiometrically limiting, such as LEM proteins (or novel partners), but not DNA (see Discussion).

## Phenotypic analysis of mutant BAFs in nuclear assembly reactions

Human and *Xenopus* BAF are nearly identical (Fig. 5 A), and had the same effects on nuclear assembly (Fig. 6). Therefore, we tested all 25 mutant human BAFs (hBAFs) in *Xenopus* nuclear assembly extracts. Each mutant was added to nuclear assembly reactions at concentrations of 0.5, 2.5, or 5 μM, incubated for 2 h, and imaged by light microscopy. BAF mutants fell into four phenotypic classes termed wild-type (decondensed-to-condensed), inactive, always condensed, and inactive-to-condensed (Fig. 8).

The wild-type class (mutants 6E, 8A, 8E, 29A, 32E, 33E, 37A, 37E, 51E, 54E, 60E, 75E, and 82E) had the same two concentration-dependent activities as wild-type BAF (Fig. 8 A). This class included all six mutations in conserved (but not identical) hBAF residues. The inactive class (mutants 25E, 25Q, 27E, 27Q, and 46E) had no detectable effects, suggesting complete loss of activity (Fig. 8 B), consistent with their lack of binding to DNA or emerin (Table I). These nuclei appeared normal by TEM (unpublished data).

The three always condensed mutants (14A, 18A, and 47E) caused chromatin to condense at all concentrations tested (Fig. 8 C). All three had normal binding to DNA (Table I), but then split into two subclasses: mutants 14A and 18A can bind emerin, but 47E cannot (Table I). We concluded that DNA (but not emerin) binding activity is required for the always condensed phenotype. When seen by TEM, nuclei assembled with low (0.5 μM) or high (5 μM) amounts of mutant 14A had thin (Fig. 9, A and F) or thick (Fig. 9, B and G) shells of condensed chromatin, respectively, and patches of double membranes. Residues 14 and

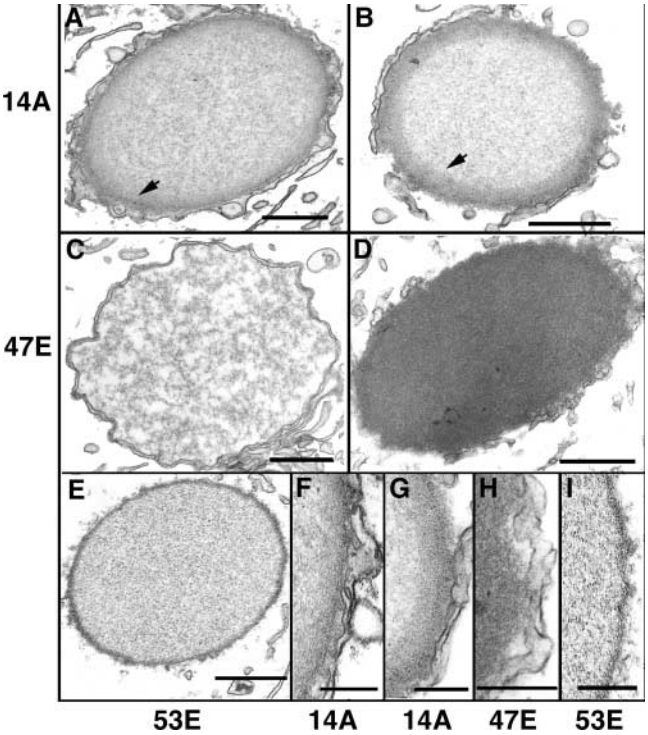


Figure 9. **TEM analysis of nuclei assembled in *Xenopus* extracts for 2 h with the indicated hBAF mutant.** (A and B) Nuclei assembled in 0.5 μM (A) or 5 μM (B) always condensed mutant 14A. Arrows indicate the thin (A) and thick (B) shell of condensed chromatin caused by this mutant. (C and D) Nuclei assembled in 0.5 μM (C) or 5 μM (D) always condensed mutant 47E; note the normal chromatin and pore-less double membrane in C, and uniformly condensed chromatin in D. (E) Nucleus assembled in 5 μM inactive-to-condensed mutant 53E. (F–I) Higher magnifications of panels A, B, D, and E. (F and G) Mutant 14A at 0.5 μM (F) and 5 μM (G). (H) Mutant 47E at 5 μM. (I) Mutant 53E at 5 μM. Bars: (A–E) 500 nm; (F–I) 200 nm.

18 define the top surface of the BAF dimer (see below). Because these mutants bind normally to both DNA and emerin, yet cause the condensed phenotype, we conclude that the top surface of BAF has a novel function.

The 47E mutant was unique. At low (0.5 μM) levels, 47E-arrested condensed nuclei had normal chromatin, and appeared to be enclosed by two parallel membranes that lacked pores (Fig. 9 C). This was distinct from nuclei growth arrested by the addition of LAP2, which accumulate NPCs (Gant et al., 1999). At high levels of 47E, chromatin had an electron-dense appearance similar to the original sperm chromatin template (Fig. 7 C), and few attached membranes, suggesting that this mutant lacked chromatin-remodelling activity.

The inactive-to-condensed class (mutants 9A, 41E, 53E, and 64E) had no effect at low concentration, but still condensed chromatin at 5 μM (Fig. 8 D). This class comprised at least two subclasses when examined by TEM, exemplified by mutants 41E (binds to DNA and emerin) and 53E (binds DNA, but not emerin). At 5 μM, mutant 41E compressed chromatin like wild-type BAF (unpublished data). The same was true for mutant 53E, except that 53E also completely abolished membrane binding to chromatin (Fig. 9, E and I). Mutant 53E, which binds DNA but not emerin, suggests that BAF binding to LEM proteins may be crucial for membrane attachment to chromatin.

### Mapping phenotypes to structure

We then mapped our results on the surface structure of the BAF dimer. Fig. 10 shows corresponding ribbon (A) and surface (B) structures of the front view of the human BAF dimer (Umland et al., 2000). In this orientation, dsDNA molecules would bind to the left and right ends, and the LEM-binding domain faces the reader. At right, the dimer is rotated down 90°C to show its top surface (Fig. 10 B).

Always condensed mutants 14A and 18A mapped between α-helices 1 and 2, and are proposed to define a novel functional surface at the top of BAF (Fig. 10 D). Not depicted are the inactive-to-condensed mutants (9A, 41E, 53E, and 64E), which mapped all over BAF, with no particular pattern (unpublished data). However, the most interesting member of this class, mutant 53E, which was selectively deficient for emerin binding and abolished membrane recruitment to chromatin, affects residue 53 in the LEM-binding valley (Fig. 10 B).

## Discussion

Our results suggest that BAF has important roles in chromatin architecture during nuclear assembly and nuclear growth, and may directly mediate chromatin condensation. Our major findings were as follows: we experimentally defined and mapped DNA- and emerin-binding residues on BAF, and residues required for dimerization; we discovered a proposed new functional surface on top of the BAF dimer; we showed that wild-type BAF has profound effects on chromatin structure during nuclear assembly; and identified an important subset of mutants (14A, 25E, 47E, and 53E) with distinct biochemical activities and phenotypes. Interestingly, wild-type BAF had either positive or negative effects on chromatin condensation, depending on BAF concentration. We propose that BAF has essential roles in chromatin attachment to membranes and chromatin decondensation during nuclear assembly.

Our current model is that LEM proteins bind centrally on the BAF dimer (as seen in Fig. 10 B, front view), whereas DNA binds to the left and right sides (Fig. 10 C). We propose that residues Pro-14 and Lys-18, on top of the BAF dimer, define a novel functional surface, because mutations at these sites had no effects on dimerization or binding to emerin or DNA, yet caused a distinct nuclear arrest phenotype (always condensed). We propose that this surface of BAF mediates either the oligomerization of BAF dimers (Zheng et al., 2000), or a novel function. Selected aspects of BAF function are discussed below.

### DNA-binding activity

We identified only four mutants (6E, 25E, 27E, and 46E) that failed to bind 200–6,000 bp dsDNA, and six mutants (9A, 25Q, 27Q, 54E, and 75E) with reduced DNA binding activity. The remaining 15 mutants bound to DNA as well as wild-type BAF in our assay, in contrast to previous reports that mutants 8E, 32E, 33E, 53E, 60E, and 64E do not bind short (21-bp) DNA fragments (Cai et al., 1998; Umland et

Downloaded from www.jcb.org on February 7, 2006

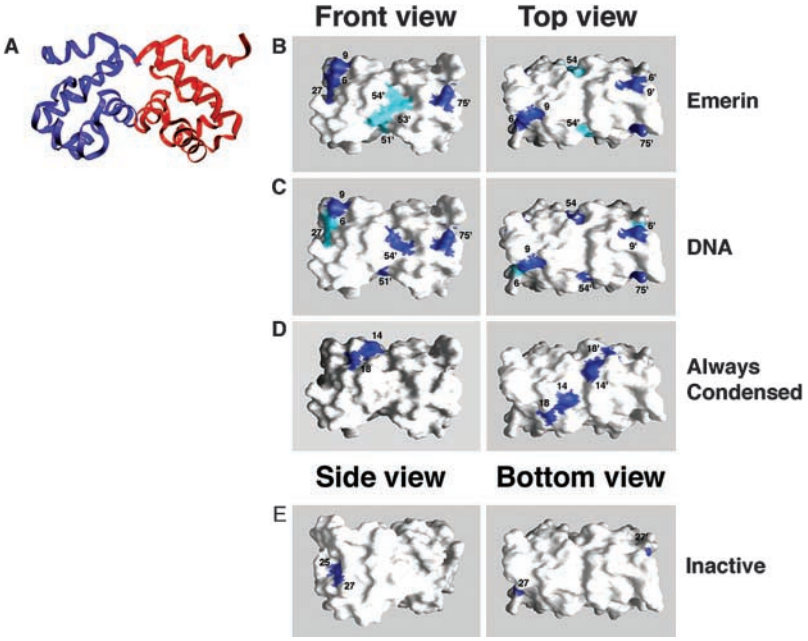


Figure 10. **Functional residues on the BAF dimer surface.** (A–C) Corresponding ribbon diagram (A) and surface structure representation (B) of the wild-type human BAF dimer (left). In the front orientation, dsDNA molecules bind to the left and right ends, and the LEM-binding domain faces the reader. The BAF dimer at right is rotated down 90° to show the top surface. Unprimed and primed numbers (e.g., 27 and 27′) indicate residues in the left and right monomers, respectively. (B) Residues essential for emerin binding are light blue: surface-exposed residues 51, 53, and 54 cluster in the valley that spans both monomers. Residues 46 and 47 (Umland et al., 2000) are buried at the dimer interface. Surface-exposed residues 6, 9, 27, and 75, in which mutations reduced (but did not eliminate) binding to emerin, are dark blue. (C) BAF residues essential for DNA binding are light blue: residues 6, 25, and 27 map to the left and right of the dimer; residue 46 is buried. Residue 25 is not visible in this front view. Surface-exposed residues 9, 51, 54, and 75, in which mutations reduced DNA binding, are dark blue. (D) Always condensed mutants mapped to the top of the dimer (residues 14 and 18), and the dimer interface (residue 47; buried). (E) Inactive mutants mapped to the left and right ends of the dimer (residues 25 and 27) and the dimer interface (residue 46; buried), as viewed from the side and bottom.

al., 2000). We attribute this difference to DNA length. In previous studies, short DNA fragments were chosen deliberately to avoid BAF-mediated DNA-bridging activity (Lee and Craigie, 1998; Zheng et al., 2000). Thus, short-DNA assays may fail to detect BAF mutants that can bind longer DNA. Our conclusions are supported by evidence that mutations at residues Lys-6 and Lys-18 do not abolish BAF's barrier-to-autointegration activity (Harris and Engelman, 2000), which requires BAF binding to retroviral DNA. We suggest that our assay identified physiologically-relevant residues required to bind DNA. Our findings point to residues 6, 25, 27, and 46 (Fig. 10 C) as critical for BAF binding to DNA. These residues map predominantly to the left and right sides of the BAF dimer (Fig. 10 C), consistent with DNA binding sites predicted from the BAF crystal structure (Umland et al., 2000).

## Model: BAF dimers have two conformational states

The three residues (51, 53, and 54) essential for binding to emerin clustered as shown in light blue (Fig. 10 B), and defined a LEM-domain binding site on the dimer. This experimentally determined LEM-binding valley is consistent with the shape and hydrophobicity of the LEM domain of LAP2, and with chemical shift mapping results (Cai et al., 2001). One major finding from our work was that all residues required to bind DNA were also important for emerin binding (see Table I). This finding supports two conformational states for BAF: a DNA-bound conformation (which enhances affinity for LEM proteins), and a DNA-free conformation. A DNA-induced conformational change in BAF was independently deduced from our previous mutational analysis of the LEM domain of LAP2; we found that a LEM domain carrying the m13 mutation could not bind BAF, but did bind BAF-DNA complexes, implying that the LEM domain sees a different BAF structure in the presence of DNA (Shumaker et al., 2001).

## BAF residues essential for binding to emerin

We identified two mutants with wild-type DNA-binding that were completely defective for emerin binding: mutants 47E and 53E (Table I). When added at 5 μM, both mutants blocked membrane attachment to chromatin, suggesting that interactions between BAF and LEM proteins may be critical for nuclear membrane recruitment during nuclear assembly. Native residue Gly-47 is buried, and our data suggest that introducing a negative charge at this site caused BAF to form weak dimers. Given that the LEM-binding site spans the dimer interface, we conclude that BAF dimerization may be essential for binding to emerin. At low concentrations, mutant 47E blocked nuclear growth even though by TEM the chromatin and enclosing nuclear membranes appeared normal, except for a possible lack of NPCs. Growth arrest by 47E could be explained by lack of nucleocytoplasmic transport. However, we do not understand how BAF might affect pore formation. Native residue Lys-53 is more easily interpretable because it is surface exposed at the predicted LEM-binding site, and the 53E mutation cleanly disrupted binding to emerin without harming protein folding, dimerization, or DNA binding. Nuclei assembled in a high concentration of either mutant 53E or 47E lacked attached membranes. These mutants, which do not bind emerin, support a model in which DNA-bound BAF must interact with LEM proteins to recruit membranes and promote chromatin decondensation and nuclear envelope growth. Note that BAF was tested for binding to only one LEM protein, emerin, in our studies. It will be interesting to determine if our BAF mutants behave identically towards LAP2 and MAN1.

Downloaded from www.jcb.org on February 7, 2006

### Inactive mutant G25E: nonfunctional in vitro, yet toxic in HeLa cells

Residues Gly-25 and Gly-27 are proposed to make crucial backbone contacts to DNA (Umland et al., 2000). DNA binding activity was abolished when Gly-25 was changed to a negatively charged Glu, consistent with charge repulsion of the DNA. As discussed above, mutant G25E was defective for all BAF functions assayed. Nonetheless, when mutant G25E is expressed in living HeLa cells, it has no apparent effect until mitosis, when it lethally disrupts nuclear assembly (Haraguchi et al., 2001). As cells progress into telophase, mutant G25E prevents wild-type BAF and emerin from localizing at the core region of telophase chromosomes, and blocks the assembly of emerin, LAP2β and lamin A (but not lamin B) at the nuclear envelope (Haraguchi et al., 2001). We speculate that living cells can somehow rescue the G25E mutant. Alternatively, the G25E mutant might retain a function for which we did not assay, such as DNA-induced oligomerization (Zheng et al., 2000), or a novel function.

### BAF localization in interphase cells

In cultured *Xenopus* cells, BAF localizes diffusely within the nucleus and concentrates near the nuclear envelope, consistent with its affinity for LEM proteins, most of which are anchored at the nuclear inner membrane. Nuclear envelope–enriched localization was not previously reported for BAF (Furukawa, 1999), but is seen in *C. elegans* embryos (unpublished data) and HeLa cells (Haraguchi et al., 2001). In telophase HeLa cells, the colocalization of BAF and emerin at specific regions on telophase chromosomes is critical for emerin to subsequently assemble at the nuclear envelope (Haraguchi et al., 2001). During interphase, BAF is also found in the nuclear interior and the cytosol. Inside the nucleus, we hypothesize that BAF interacts with LAP2α, an abundant soluble (not membrane anchored) LEM protein that binds lamin A (Dechat et al., 1998, 2000a, 2000b). However, LAP2α fragments that lack the LEM domain localize normally in HeLa cells (Dechat et al., 1998), so the in vivo role of BAF with respect to LAP2α is not known. We also found BAF in the cytoplasm of cultured cells, consistent with the purification of BAF activity from the cytosol of NIH-3T3 cells (Lee and Craigie, 1998). Although BAF is small, it seems unlikely that it would diffuse out of the nucleus, unless its DNA- and LEM-binding activities were inhibited. Our results neither address nor explain the potential roles of cytoplasmic BAF.

### Enhanced chromatin decondensation and nuclear growth: regulated BAF activity?

We are intrigued by the enhanced chromatin decondensation and nuclear growth caused by adding 4% extra BAF to assembling nuclei. We propose that these positive effects are due to regulated interactions with endogenous LEM proteins. We hypothesize that properly regulated BAF has positive roles during nuclear assembly, in promoting membrane attachment, chromatin decondensation, and nuclear growth. We further propose that adding 20% extra BAF to assembling nuclei might saturate endogenous LEM proteins, or novel regulatory partner(s), and lead to unregulated (inherently compressive?) BAF interactions with DNA. Other models are also possible. Our results support the idea that a fundamental function of BAF is to bind LEM proteins during nuclear assembly, and thereby attach chromatin to the nuclear inner membrane. In the nuclear interior, BAF interactions with soluble lamin-binding LEM proteins (such as LAP2α) might link chromatin to intranuclear lamins. Our structure–function analysis of BAF, and the subset of biochemically-distinct BAF mutants (14A, 18A, 25E, 47E, and 53E) identified here, will provide a useful foundation for understanding this highly-conserved chromatin protein.

## Materials and methods

### *Xenopus* extracts and assembly reactions

Assembly extracts were prepared by centrifugation at 200,000 *g* as described (Newmeyer and Wilson, 1991). To assemble nuclei, membranes and cytosol were thawed and mixed on ice, with or without recombinant BAF protein, and then supplemented with demembranated *Xenopus* sperm chromatin (Lohka and Masui, 1983) to a final concentration of 1,000–1,500 units/μl. A typical reaction contained 10 μl cytosol, 1 μl membranes, 1 μl recombinant BAF protein, and 0.5 μl chromatin. The recombinant protein added did not exceed 20% of the final volume. Assembly was initiated by incubating at 22–25°C. At each timepoint, aliquots were removed, stained for DNA and fixed by adding 10 μg/ml Hoechst 33342 dye in 3.7% formaldehyde. Samples were coverslipped and imaged using a Nikon Microphot microscope with a Photometrics SenSys camera and IPLab software (Scanalytics).

### Site-directed mutagenesis of human BAF

The cDNA encoding human BAF in the pET15b vector (Novagen, Inc.; Lee and Craigie, 1998) was mutagenized using the Quickchange site-directed mutagenesis kit (Stratagene, Inc.). For alanine-substitution mutagenesis, the entire plasmid was replicated by PCR using a pair of complementary mutagenic oligonucleotides as primers to replace the indicated residue with alanine (Fig. 1). Each primer included 6–24 nucleotides of perfect homology flanking the region to be mutated. The original DNA strands were destroyed by digestion with *Dpn*I (Stratagene, Inc.), and the mutated DNA was transformed into *Escherichia coli* XL-1-blue cells. All mutations were verified by full-length dsDNA sequencing (unpublished data). Charge substitution mutations in BAF were described previously by Cai et al. (1998).

### Recombinant BAF proteins

His-tagged BAF proteins were expressed in *E. coli* and purified essentially as described (Lee and Craigie, 1998), but were not dimer-purified and therefore also contained oligomeric BAF complexes (Zheng et al., 2000). For a detailed protocol for BAF purification, contact the corresponding author.

### Synthesis of $^{35}$S-Cys/Met-labeled proteins

BAF proteins lacking the six-His tag were produced synthetically using coupled transcription and translation reactions (Promega Corp.). Template DNA was first amplified by PCR from plasmid DNA, using a 5′ primer that contained a T7 promoter site and Kozak consensus sequence to drive protein expression in vitro, plus the first 20 nucleotides of the BAF open reading frame (5′-GATCCTAATACGACTCACTATAGGGAACAGCCACCATGACAACCTCCCAAAAGCA-3′). Our 3′primer comprised a poly $(A)_{30}$ tail and the last 20 nucleotides of the cDNA sequence encoding BAF (5′-T[30]TCACAAGAAGGCGTCGCACC-3′). Proteins with a six-His tag were made using the plasmid DNA template (pET15b vector), which has a T7 promoter. A typical TNT reaction contained 40 μl reaction mix, 5 μl PCR-generated template DNA or 1 μg plasmid DNA, 2 μl $^{35}$S Ready Pro-Mix (Amersham Biosciences), and nuclease-free water for a final volume of 50 μl.

### BAF binding to emerin

A cDNA encoding wild-type emerin residues 1–222 in the pET11c vector (Novagen Inc.; Lee et al., 2001) was transformed into *E. coli* strain BL21 (DE3). Cells with this plasmid were grown to an $OD_{600}$ of 0.6, and emerin expression was induced by 0.4 mM IPTG for 4 h. Cells were pelleted 5 min at 14,000 *g*, and resuspended in 2 × SDS sample buffer. Proteins from unfractionated bacterial lysates were separated on 10% SDS-PAGE gels,

Downloaded from www.jcb.org on February 7, 2006

transferred to Immobilon-P PVDF membrane (Millipore Corp.), and blocked for 1 h in PBST containing 5% nonfat dry milk. Blots were washed twice in BRB (Blot Rinse Buffer; 10 mM Tris-HCl, pH 7.4, 150 mM NaCl, 1 mM EDTA, 0.1% Tween-20) for 5 min at 22–24°C, and incubated with 5 μl $^{35}$S-cysteine/methionine-labeled probe protein (wild-type or mutant BAF) diluted 1:200 into BRB containing 0.1% fetal calf serum (final volume, 1 ml). Blots were incubated at 4°C overnight with the $^{35}$S-labeled in vitro–transcribed/translated probe protein, washed four times in BRB, dried and exposed to Hyperfilm MP (Amersham Biosciences).

### Subunit exchange with wild-type BAF

$^{35}$S-labeled wild-type BAF was mixed with each His-tagged mutant BAF, and interactions were assayed by coimmunoprecipitation. Specifically, $^{35}$S-labeled wild-type BAF protein (10 μl) was incubated with 500 ng unlabeled recombinant (wild-type or mutant) BAF protein for 30 min at 22–24°C. We then added 300 μl of cold immunoprecipitation buffer (20 mM Hepes, pH 7.9, 150 mM NaCl, 10 mM EDTA, 2 mM EGTA, 0.1% Nonidet P-40, 10% glycerol, 1 mM DTT, 1 mM PMSF, and 20 ug/ml each aprotinin and leupeptin), plus 5 μl of anti-His rabbit polyclonal antibody (sc-803; Santa Cruz Biotechnology), and incubated at 4°C with constant mixing for 1 h. We then added 50 μl washed protein A Sepharose beads (Amersham Biosciences), incubated overnight at 4°C, centrifuged at 5,000 *g* for 5 min to pellet the beads, and washed pellets five times with ice-cold IP buffer. Bound proteins were removed from beads by boiling in 40 μl 2 × SDS sample buffer, subjected to SDS-PAGE on 4–12% gradient gels (Invitrogen Corp.), dried and exposed to Hyperfilm MP (Amersham Biosciences).

### BAF binding to native DNA cellulose beads

DNA binding assays were performed as described (Kasof et al., 1999), with the following modifications. The $^{35}$S-labeled wild-type or mutant BAF protein (9 μl of a 50 μl TNT reaction; see above) was first incubated with 200 μl of NETN buffer (20 mM Tris, pH 8, 100 mM NaCl, 1 mM EDTA, 0.2% Nonidet P-40) and 50 μl native DNA cellulose beads (Amersham Biosciences) for either 2 h (or overnight) at 4°C. Samples were then washed four times in NETN, resolved by SDS-PAGE, dried and visualized by autoradiography.

### Circular dichroism spectroscopy

We used a Jasco J720 spectrometer (Jasco) at 22–24°C to measure spectra in the far UV region (200–260 nm) at a protein concentration of 0.75 mg/ml in a quartz cuvette with a 100-nm path length.

### Size exclusion chromatography

We used a Superdex 25 column (HR 3.2/30; Amersham Biosciences) on an Amersham Pharmacia Smart System. The column was equilibrated and run with 20 mM Tris, pH 7.5, 150 mM NaCl, 5 mM DTT, 0.1 mM EDTA and 10% (wt/vol) glycerol. Protein (40 ml) was loaded at a concentration of 0.2 mg/ml and eluted at a flow rate of 50 ml/min.

### Cloning of *Xenopus* BAF

A BLAST search with the human BAF cDNA yielded an EST with high homology in *Xenopus laevis*. This clone (GenBamk/EMBL/DDBJ accession no. AW641186) was obtained from Research Genetics, Inc. A full-length *Xenopus* BAF (xBAF) ORF was amplified by PCR from this clone using a 28-base 5′ primer with an *Nde*I restriction site and a 30-base 3′ primer with a *Bam*HI site, and cloned into the *Nde*I and *Bam*HI sites of the pET15b vector (Novagen Inc.). The insert was verified by double-stranded DNA sequencing (unpublished data).

### BAF antibodies, immunoblotting, and indirect immunofluorescence

A peptide comprising residues 19-35 of xBAF (KSVQCLAGIGEALGHRL) was synthesized by Boston Biomolecules, and rabbit polyclonal antiserum was produced by Covance, Inc., in rabbit 3710, using as antigen the KLH-conjugated peptide. BAF antiserum 3710 was affinity purified by binding the BAF peptide (Reduce-Imm Reducing Kit and Sulfolink Kit, Pierce Chemical Co.), and used at dilutions of 1:100 for blots and 1:10 for indirect immunofluorescence (below).

For immunoblots, proteins were loaded onto 4-12% NuPAGE gels (Invitrogen Corp.), electrophoresed, and transferred onto Immobilon-P PVDF membranes for 30 min. Blots were blocked for 1 h at 25°C in PBS containing 0.1% Tween 20 (PBST) and 5% nonfat dry milk. Subsequent incubations in primary and secondary antibodies were done in PBST. xBAF was detected on blots using a 1:2,000 dilution of crude rabbit polyclonal serum 3710, or 1:100 dilution of affinity-purified serum 3710. Blots were incubated with primary antibody for 1 h at 25°C (or overnight at 4°C), washed in PBST for 20 min three times, followed by horseradish peroxidase-conjugated goat anti–rabbit antibodies (1:50,000 dilution; Pierce Chemical Co.), then washed in PBST for 20 min three times. Proteins were visualized by enhanced chemiluminescence and exposure to Hyperfilm MP (Amersham Biosciences).

For indirect immunofluorescence of cultured *Xenopus* epithelial cells (A6 and XLK-WG lines), cells were fixed in 4% paraformaldehyde and washed in PBS containing 0.1% Tween 20 and 1% bovine serum albumin. The *Xenopus* kidney epithelial cells (XLK-WG line; pseudodiploid) were a gift from Dr. Joe Gall (Carnegie Institute, Baltimore, MD).

### Immunofluorescence of in vitro assembled nuclei

Aliquots (5 μl) of 12 μl nuclear assembly reactions were placed on a microscope slide coated with 0.1% polylysine, coverslipped, and flash frozen in liquid nitrogen. Samples were then fixed at –20°C in methanol then acetone (20 min each). Slides were placed in 0.1% PBST and 5% milk for 10 min, and then rinsed quickly in PBST. Slides were incubated for 30 min at 22–24°C with 50 μl primary antibody (peptide-purified serum 3710 against xBAF, or mAb S49 against *Xenopus* lamin $B_3$, a gift of R. Stick [Bremen University, Bremen, Germany]) diluted to 1:25 and 1:100 in PBS, respectively. Slides were then washed with PBS three times (10 min each), incubated 30 min with a 1:250 dilution of the fluorochrome-labeled secondary antibody, washed in PBS three times (10 min each), and mounted with 10 μg/ml Hoechst 33342 dye in 3.7% formaldehyde.

### Quantitation of endogenous BAF in *Xenopus* egg cytosol

Various amounts (1, 2, 4, and 8 μl) of a 1:10 dilution of *Xenopus* egg cytosol were compared with purified recombinant xBAF (5, 10, 20, 40, and 80 ng) on western blots. Samples were immunoblotted as described above, probed with affinity-purified 3710 antibodies and alkaline phosphatase-conjugated donkey anti–rabbit antibody (1:1,000 dilution; Jackson ImmunoResearch Laboratories), and visualized by a colorimetric reaction (AP conjugate substrate kit; BioRad Laboratories). Blots were quantitated using FluorChem v.2 software (Alpha Innotech, Corp.). Intensities for known amounts of recombinant BAF were plotted as a standard curve using the Sigma Plot software (Jandel Scientific). The intensity of BAF in 1 μl diluted cytosol fell within the linear range of detection, and the amount of endogenous BAF was calculated from the standard curve. The *Xenopus* egg cytosol fraction contains 25 μM monomeric BAF, or 12.5 μM BAF dimers.

### Structural modeling of BAF

Residues were mapped using coordinates for the crystal structure of BAF (PDB Id: 1CI4; Umland et al., 2000). BAF was manipulated using the GRASP program (A. Nicholls, Department of Biochemistry and Molecular Biophysics, Columbia University, New York).

### Transmission EM

*Xenopus* nuclear assembly reactions (100 μl) were fixed by mixing with 700 μl membrane wash buffer (MWB: 250 mM sucrose, 50 mM KCl, 2.5 mM $MgCl_2$, 50 mM Hepes, pH 8, 1 mM ATP) plus 700 μl 2× fix buffer (250 mM sucrose, 100 mM Hepes, pH 8, 1.5 mM $MgCl_2$, 1.5 mM $CaCl_2$, 1% glutaraldehyde, 0.5% paraformaldehyde), and incubating 20 min at 22–25°C. Samples were then pelleted in a horizontal microcentrifuge (Beckman Microfuge E™) for 1 min at full speed (14,000 rpm), and washed three times (5 min each) in cacodylate buffer (0.2 M cacodylate, pH 7.4, 1.5 mM $MgCl_2$, 1.5 mM $CaCl_2$). Samples were then fixed 1 h in cacodylate buffer containing 4% reduced osmium ($OsO_4$), washed twice (5 min each) in distilled water, and stained 20 min in 1% uranyl acetate in distilled water. Samples were dehydrated by a graded series of 5 min incubations in 50, 70, and 90% ethanol, followed by three 3-min incubations in 100% ethanol. Samples were then embedded in Spurr's medium, sectioned (80–120 nm thick), and visualized using a Philips CM120 transmission electron microscope.

### Supplemental materials available

Fig. S1 (available at http://www.jcb.org/cgi/content/full/jcb.200202019/DC1) shows immunofluorescence staining for BAF and lamins in nuclei assembled in 5 μM added exogenous wild-type BAF.

We thank Jose Luis Avalos for help with the three-dimensional structural programs, and Sheona Drummond for help with immunofluorescence. We are grateful to Kenneth Lee, Yosef Gruenbaum, and Tokuko Haraguchi for stimulating discussions and comments on this manuscript.

This work was funded by a National Institutes of Health grant (RO1 GM48646) to K.L. Wilson.

Downloaded from www.jcb.org on February 7, 2006

Submitted: 6 February 2002
Revised: 28 May 2002
Accepted: 11 June 2002

## References

Berger, R., L. Theodor, J. Shoham, E. Gokkel, F. Brok-Simoni, K.B. Avraham, N.G. Copeland, N.A. Jenkins, G. Rechavi, and A.J. Simon. 1996. The characterization and localization of the mouse thymopoietin/lamina-associated polypeptide 2 gene and its alternatively spliced products. *Genome Res.* 6:361–370.

Boman, A.L., M.R. Delannoy, and K.L. Wilson. 1992. GTP hydrolysis is required for vesicle fusion during nuclear envelope assembly in vitro. *J. Cell Biol.* 16: 281–294.

Cai, M., Y. Huang, R. Zheng, S.Q. Wei, R. Ghirlando, M.S. Lee, R. Craigie, A.M. Gronenborn, and G.M. Clore. 1998. Solution structure of the cellular factor BAF responsible for protecting retroviral DNA from autointegration. *Nat. Struc. Biol.* 5:903–909.

Cai, M., Y. Huang, R. Ghirlando, K.L. Wilson, R. Craigie, and G.M. Clore. 2001. Solution structure of the constant region of nuclear envelope protein LAP2 reveals two LEM-domain structures: one binds BAF and the other binds DNA. *EMBO J.* 20:4399–407.

Chen, H., and A. Engelman. 1998. The barrier-to-autointegration protein is a host factor for HIV type 1 integration. *Proc. Natl. Acad. Sci. USA*. 95:15270–15274.

Clements, L., S. Manilal, D.R. Love, and G.E. Morris. 2000. Direct interaction between emerin and lamin A. *Biochem. Biophys. Res. Commun*. 267:709–714.

Cohen, M., K.K. Lee, K.L. Wilson, and Y. Gruenbaum. 2001. Transcriptional repression, apoptosis, human disease and the functional evolution of the nuclear lamina. *Trends Biochem. Sci*. 26:41–47.

Dechat, T., J. Gotzmann, A. Stockinger, C. Harris, M.A. Talle, J.J. Siekierka, and R. Foisner. 1998. Detergent-salt resistance of LAP2alpha in interphase nuclei and phosphorylation-dependent association with chromosomes early in nuclear assembly implies functions in nuclear structure dynamics. *EMBO J.* 17:4887–4902.

Dechat, T., B. Korbei, O.A. Vaughan, S. Vlcek, C.J. Hutchison, and R. Foisner. 2000a. Lamina-associated polypeptide 2alpha binds intranuclear A-type lamins. *J. Cell Sci*. 113:3473–3484.

Dechat, T., S. Vlcek, and R. Foisner. 2000b. Review: lamina-associated polypeptide 2 isoforms and related proteins in cell cycle-dependent nuclear structure dynamics. *J. Struct. Biol.* 129:335–345.

Foisner, R., and L. Gerace. 1993. Integral membrane proteins of the nuclear envelope interact with lamins and chromosomes, and binding is modulated by mitotic phosphorylation. *Cell*. 73:1267–1279.

Furukawa, K. 1999. LAP2 binding protein 1 (L2BP1/BAF) is a candidate mediator of LAP2- chromatin interaction. *J. Cell Sci.* 112:2485–2492.

Gant, T.M., C.A. Harris, and K.L. Wilson. 1999. Roles of LAP2 proteins in nuclear assembly and DNA replication: truncated LAP2beta proteins alter lamina assembly, envelope formation, nuclear size, and DNA replication efficiency in *Xenopus laevis* extracts. *J. Cell Biol.* 144:1083–1096.

Goldberg, M., H. Lu, N. Stuurman, R. Ashery Padan, A.M. Weiss, J. Yu, D. Bhattacharyya, P.A. Fisher, Y. Gruenbaum, and M.F. Wolfner. 1998. Interactions among *Drosophila* nuclear envelope proteins lamin, otefin, and YA. *Mol. Cell. Biol.* 18:4315–4323.

Haraguchi, T., T. Koujin, M. Segura-Totten, K.K. Lee, Y. Matsuoka, Y. Yoneda, K.L. Wilson, and Y. Hiraoka. 2001. BAF is required for emerin assembly into the reforming nuclear envelope. *J. Cell Sci*. 114: 4575–4585.

Harris, D., and A. Engelman. 2000. Both the structure and DNA binding function of the barrier-to-autointegration factor contribute to reconstitution of HIV type 1 integration in vitro. *J. Biol. Chem.* 275:39671–39677.

Kasof, G.M., L. Goyal, and E. White. 1999. Btf, a novel death-promoting transcriptional repressor that interacts with Bcl-2 related proteins. *Mol. Cell Biol*. 19:4390–4404.

Lee, K.K., Y. Gruenbaum, P. Spann, J. Liu, and K.L. Wilson. 2000. *C. elegans* nuclear envelope proteins emerin, MAN1, lamin, and nucleoporins reveal unique timing of nuclear envelope breakdown during mitosis. *Mol. Biol Cell*. 11:3089–3099.

Lee, K.K., T. Haraguchi, R.S. Lee, T. Koujin, Y. Hiraoka, and K.L. Wilson. 2001. Distinct functional domains in emerin bind lamin A and DNA-bridging protein BAF. *J. Cell Sci.* 114:4567–4573.

Lee, M.S., and R. Craigie. 1998. A previously unidentified host protein protects retroviral DNA from autointegration. *Proc. Natl. Acad. Sci. USA*. 95:1528–1533.

Lin, F., D.L. Blake, I. Callebaut, I.S. Skerjanc, L. Holmer, M.W. McBurney, M. Paulin-Levasseur, and H.J. Worman. 2000. MAN1, an inner nuclear membrane protein that shares the LEM domain with lamina-associated polypeptide 2 and emerin. *J. Biol. Chem*. 275:4840–4847.

Lohka, M.J., and Y. Masui. 1983. Formation in vitro of sperm pronuclei and mitotic chromosomes induced by amphibian ooplasmic components. *Science*. 220:719–721.

Meier, E., B.R. Miller, and D.J. Forbes. 1995. Nuclear pore complex assembly studied with a biochemical assay for annulate lamellae formation. *J. Cell Biol*. 129:1459–1472.

Newmeyer, D.D., and K.L. Wilson. 1991. Egg extracts for nuclear import and nuclear assembly reactions. *Meth. Cell Biol*. 36:607–634.

Philpott, A., G.H. Leno, and R.A. Laskey. 1991. Sperm decondensation in Xenopus egg cytoplasm is mediated by nucleoplasmin. *Cell*. 65:569–578.

Shao, X., and N. Grishin. 2000. Common fold in helix-hairpin-helix proteins. *Nuc. Acids Res*. 28:2643–2650.

Shumaker, D.K., K.K. Lee, Y.C. Tanhehco, R. Craigie, and K.L. Wilson. 2001. LAP2 binds to BAF-DNA complexes: requirement for the LEM domain and modulation by variable regions. *EMBO J*. 20:1754–1764.

Stuurman, N., S. Heins, and U. Aebi. 1998. Nuclear lamins: their structure, assembly, and interactions. *J. Struct. Biol*. 122:42–66.

Umland, T.C., S.-Q. Wei, R. Craigie, and D.R. Davies. 2000. Structural basis of DNA bridging by barrier-to-autointegration factor. *Biochemistry*. 39:9130–9138.

Vaughan, O.A., M. Alvarez-Reyes, J.M. Bridger, J.L.V. Broers, F.C. Ramaekers, M. Wehnert, G.E. Morris, W.G.F. Whitfield, and C.J. Hutchinson. 2001. Both emerin and lamin C depend on lamin A localization at the nuclear envelope. *J. Cell Sci.* 114:2577–2590.

Wilson, K.L., and J. Newport. 1988. A trypsin-sensitive receptor on membrane vesicles is required for nuclear envelope formation in vitro. *J. Cell Biol.* 107: 57–68.

Wolff, N., B. Gilquin, K. Courchay, I. Callebaut, H.J. Worman, and S. Zinn-Justin. 2001. Structural analysis of emerin, an inner nuclear membrane protein mutated in X-linked Emery-Dreifuss muscular dystrophy. *FEBS Lett*. 501: 171–176.

Woodland, H., and E. Adamson. 1977. The synthesis and storage of histones during the oogenesis of *Xenopus laevis*. *Dev Biol*. 57:118–135.

Zheng, R., R. Ghirlando, M.S. Lee, K. Mizuuchi, M. Krause, and R. Craigie. 2000. Barrier-to-autointegration factor (BAF) bridges DNA in a discrete, higher-order nucleoprotein complex. *Proc. Natl. Acad. Sci USA*. 97:8997–9002.

Downloaded from www.jcb.org on February 7, 2006